

Comparison of penetration depth between two-photon excitation and single-photon excitation in imaging through turbid tissue media

Min Gu,^{a)} Xiaosong Gan, Aernout Kisteman and Ming Gun Xu
*Centre for Micro-Photonics, School of Biophysical Sciences and Electrical Engineering,
 Swinburne University of Technology, PO Box 218, Hawthorn 3122, Victoria, Australia*

(Received 8 March 2000; accepted for publication 18 July 2000)

We show, both theoretically and experimentally, that for a turbid tissue medium where Mie scattering is dominant, multiple scattering not only reduces the illumination power in the forward direction but also exhibits an anisotropic distribution of scattered photons. Thus, a signal level under two-photon excitation drops much faster than that under single-photon excitation although image resolution is much higher in the former case. As a result, the penetration depth under two-photon excitation is limited by the strength of two-photon fluorescence and is not necessarily larger than that under single-photon excitation. © 2000 American Institute of Physics.

[S0003-6951(00)04536-8]

Two-photon (2p) scanning fluorescence microscopy has been widely used in various fields^{1,2} because this technology has proven advantageous over single-photon (1p) scanning fluorescence microscopy. First, 2p excitation is a nonlinear process¹ and therefore the fluorescence intensity is directly proportional to the square of the excitation intensity. Due to this quadratic dependence, the 2p imaging technique provides a pinpoint excitation/detection method at a deep position within thick samples. Second, if an infrared laser beam is employed for 2p excitation, 2p fluorescence microscopy offers access to ultraviolet (UV) excitation without using UV lasers, and reduces Rayleigh scattering appreciably provided that the size of scatterers in tissue is much smaller than the illumination wavelength. According to these properties of 2p excitation, it has been claimed that 2p excitation results in a deeper penetration depth than 1p excitation.^{1,2}

Recently, 2p fluorescence microscopy has been used in imaging through thick tissue²⁻⁷ for photodynamic therapy and early detection of small tumors. Biological tissue is usually composed of small scatterers such as bacteria, viruses, malignant cells and so on. The size of these scatterers varies from 0.1 μm to a few micrometers.^{8,9} Therefore, the dominant scattering effect caused by these scatterers is Mie scattering rather than Rayleigh scattering. The physical difference between these two types of scattering is that the former is anisotropic scattering whereas the latter is isotropic scattering.¹⁰ The strength of Rayleigh scattering is inversely proportional to the fourth power of the illumination wavelength. However, Mie scattering exhibits a more complicated nature as shown in Fig. 1.

Figure 1 shows the scattering efficiency Q , which is defined as the ratio of the scattering cross section σ_s to the geometrical cross section, and the anisotropy value g in Mie scattering as a function of the scattering parameter A (A is defined as the ratio of the size of a scattering particle a to the light wavelength λ).¹⁰ It is seen from this example that, for a given scatterer size, Q and g decrease with the illumination wavelength if A is approximately less than one. The decrease

in the scattering efficiency implies a reduction of multiple scattering events, which leads to high image resolution and signal level in microscopy imaging.¹¹ However the decrease in the anisotropy value results in a broad distribution of scattered photons in the focal region,¹¹ which may reduce the image resolution and signal level.¹¹ The competition of these two processes, together with the quadratic dependence of the 2p fluorescence intensity, determines the limiting factor on penetration depth.

To demonstrate the limiting factor on the penetration depth under 2p and 1p excitation, we consider a turbid medium consisting of scattering particles (diameters of 0.202 μm) suspended in water. The turbid medium was placed in a glass cell with lateral dimensions of 2 cm \times 1 cm. The thickness, d , of the glass cell was varied from 25 up to 250 μm which is the maximum working distance of the objective used in experiments.

A uniform fluorescent polymer bar¹² was embedded at the bottom of the glass cell. The fluorescent bar can be excited under 1p ($\lambda_s=488\text{ nm}$) and 2p ($\lambda_i=800\text{ nm}$) excitation¹² with a peak fluorescence wavelength approximately at 520 nm. Due to the different wavelengths associated with 1p excitation, 2p excitation and fluorescence, the

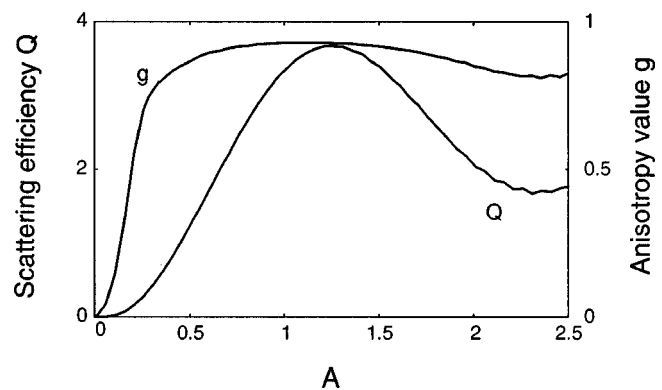


FIG. 1. Scattering efficiency Q and anisotropy value g in Mie scattering as a function of the scattering parameter A . The refractive indices of scatterers (spherical particles) and the immersion medium (water) are 1.59 and 1.33, respectively.

^{a)}Electronic mail: mgu@swin.edu.au

TABLE I. Calculated values of the scattering cross section σ_s , the scattering-mean-free-path length l_s , and the anisotropy value g for polystyrene beads $0.202 \mu\text{m}$ in diameter at wavelengths of 488, 520 and 800 nm, respectively, for a given particle weight concentration of 2.5%. The geometric cross section of the scatterers is $0.032 \mu\text{m}^2$.

Wavelength (nm)	Relative particle size, A (a/λ)	Scattering efficiency, $Q_s = \sigma_s/\sigma_g$	Scattering cross section, σ_s (μm^2)	SMFP length, l_s (μm)	Anisotropy value, g
488	0.2069	0.1586	5.07×10^{-3}	35.7	0.54
520	0.1942	0.1356	4.34×10^{-3}	41.8	0.482
800	0.1263	0.0389	1.24×10^{-3}	145.38	0.20

scattering cross section σ_s , the scattering mean-free-path (SMFP) length l_s and the anisotropy value g are different and can be calculated using Mie scattering theory¹⁰ (Table I).

The prepared sample cell was placed under an Olympus confocal scanning microscope (Flouview).⁵ For 1p excitation, an Ar ion laser at a wavelength of 488 nm was used. A Spectra-Physics ultrashort pulsed laser (Tsunami) with a pulse width of 80 fs was employed for 2p excitation at 800 nm wavelength.⁵ To avoid the effect of refractive-index mismatching between the turbid medium and the cover glass of the cell, a water-immersion objective (Olympus UplanApo 60 \times , $\infty/1.13$ –0.21, numerical aperture=1.2, working distance=250 μm) was used. In the case of 1p excitation, a pinhole 300 μm (optical unit ~ 3) in diameter was placed in front of the detector to produce an optical sectioning effect with strength similar to that under 2p excitation without using a pinhole.^{1,13} This arrangement implies that the ability of rejecting scattered photons caused by the optical sectioning effect is the same in the two cases.¹⁴

Figure 2 shows the dependence of the measured fluorescence signal level on the sample thickness d under 1p and 2p excitation. The signal level has been normalized by the fluorescence signal measured without the turbid medium ($d=0$). Such normalization is equivalent to the assumption that the fluorescence intensity at $d=0$ is the same under 1p and 2p excitation and provides a benchmark for comparison between the two cases. It is seen that the 2p fluorescence signal level is better than the 1p fluorescence signal level when d is less than the 1p SMFP. After that depth, the 2p fluorescence signal level drops much more quickly than the 1p fluorescence signal level. For example, at $d=225 \mu\text{m}$, the

former is approximately two orders of magnitude lower than the latter. To confirm this measured dependence, we used the Monte Carlo simulation method,¹⁵ which is based on Mie scattering theory,¹⁰ to calculate the signal levels. The theoretical prediction shown in Fig. 2 agrees with the experimental results in the sense that the 2p fluorescence signal level is lower than the 1p fluorescence signal level.

To understand the phenomenon in Fig. 2, we should point out that both unscattered and scattered illumination photons can contribute to fluorescence emission. However, the fluorescence contributed by these two groups of photons behaves in different ways between 2p and 1p excitation.

We first consider the case where the thickness d is less than the 1p SMFP length. In this case, the number of unscattered illumination photons is considerable in the total number of photons but decreases exponentially with d/l_s . In other words, the logarithm of the emitted fluorescence signal contributed by unscattered illumination photons decreases linearly with d , as observed in Fig. 2. Due to the quadratic dependence of 2p fluorescence on the illumination intensity, the number of 2p fluorescence photons produced by the unscattered illumination photons decreases exponentially with $2d/l_s$. As a result, for a given depth d , the 2p fluorescence signal excited by the unscattered illumination photons is stronger, because the 2p SMFP length is approximately four times as large as that for 1p excitation (Table I).

When d becomes larger than the 1p SMFP length, the 2p fluorescence signal still decreases exponentially with $2d/l_s$ but scattered illumination photons make a significant contribution to the generation of 1p fluorescence. As a result, the dropping of 1p fluorescence becomes slower than that of 2p fluorescence.

Once the thickness d is larger than the 2p SMFP length, scattered photons play a dominant role in the excitation and emission processes. In general, scattered photons distribute in a broad region near the geometric focus.¹¹ Because of the lower anisotropy value g and the larger l_s value, the scattered illumination photons under 2p excitation distribute in a boarder region than those under 1p excitation. This feature results in a lower photon density near the geometric focus. Therefore, the 2p fluorescence emission excited by scattered photons is less efficient than the 1p fluorescence emission. Further, due to the quadratic dependence under 2p excitation, 2p fluorescence emission excited by scattered illumination photons becomes even less efficient. In addition, 2p fluorescence photons excited by scattered illumination photons have less of a possibility of reaching the detector because they originate from a broader region. As a result, 2p fluorescence

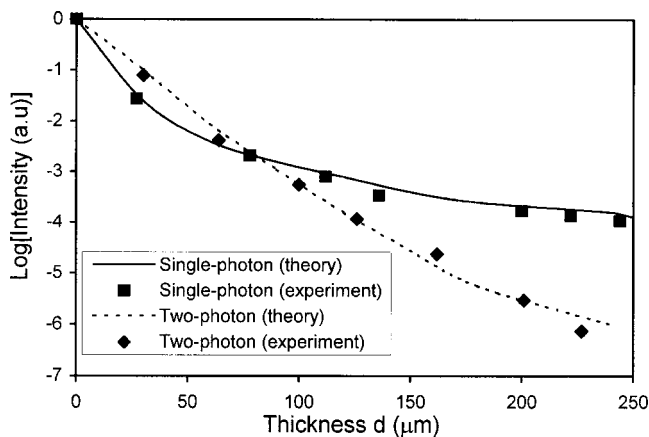


FIG. 2. Signal level under 2p and 1p excitation as a function of the penetration depth in a turbid medium consisting of scatterers $0.202 \mu\text{m}$ in diameter.

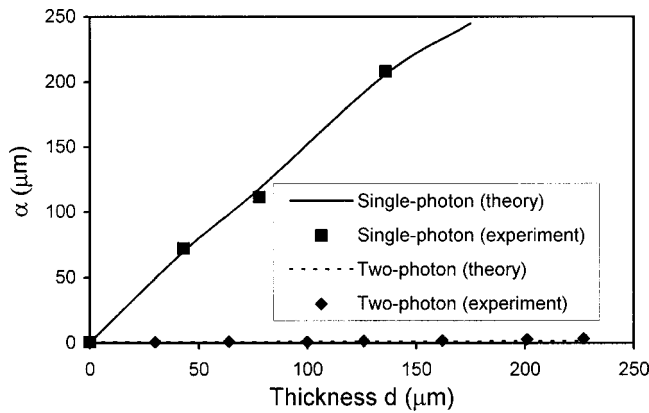


FIG. 3. Image resolution under 2p and 1p excitation as a function of the penetration depth of a turbid medium consisting of scatterers $0.202 \mu\text{m}$ in diameter.

produced by the scattered illumination photons exhibits a lower signal level than 1p fluorescence.

However the stronger suppression of the contributions from scattered illumination and fluorescence photons under 2p excitation may be advantageous in terms of image resolution. To confirm this, we measured the transverse edge image of the fluorescence polymer bar. Image resolution α is defined as the distance between the 10% and 90% intensity points, measured from the edge responses after they are fitted. The dependence of resolution α on sample thickness d is depicted in Fig. 3 which also includes the Monte Carlo simulation results corresponding to the experimental condition. A good agreement between the experiments and theoretical predictions is observed. For the turbid medium we used, the image resolution under 2p excitation is two orders of magnitude higher than that under 1p excitation.

Experiments similar to Figs. 2 and 3 were also carried out for different sizes of scatterers. In general, the smaller the scatterer size (the smaller the anisotropy value and the larger the SMFP length), the quicker the reduction of the 2p fluorescence signal. Based on this property, we can conclude

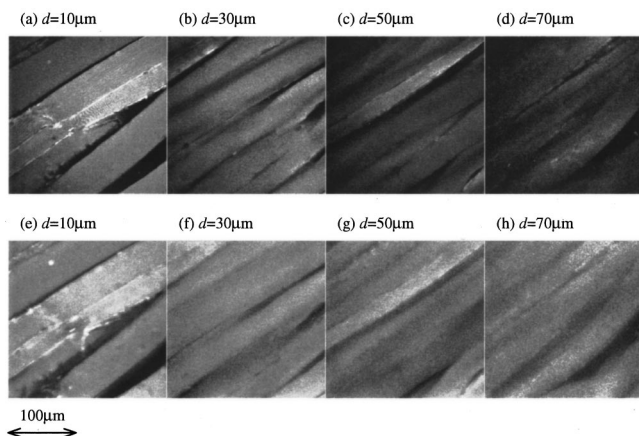


FIG. 4. Measured transverse (x - y) images through a thick muscle tissue sample under 2p and 1p excitation. (a)–(d) 2p fluorescence images at depths of 10, 30, 50, and $70 \mu\text{m}$; (e)–(h) 1p fluorescence images at depths of 10, 30, 50, and $70 \mu\text{m}$.

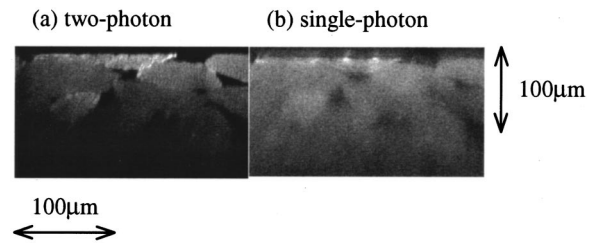


FIG. 5. Measured axial (x - z) images through a thick muscle tissue sample under (a) 2p and (b) 1p excitation.

that, for a real tissue medium consisting of different size Mie scatterers, the 2p fluorescence signal level is lower than the 1p signal level at a deep depth. This conclusion is demonstrated in Figs. 4 and 5.

Figures 4 and 5 show the transverse (x - y) and axial (x - z) autofluorescence images of muscle tissue under 2p ($\lambda_i = 800 \text{ nm}$) and 1p ($\lambda_i = 488 \text{ nm}$) excitation. The image intensity has been normalized by the maximum intensity at the surface of the sample. The muscle tissue has an average 1p SMFP length of approximately $20 \mu\text{m}$.⁸ The 2p transverse images [Figs. 4(a)–4(d)] were recorded at depths of 10, 30, 50, and $70 \mu\text{m}$, and show a higher resolution but become significantly weaker at a deeper depth than the 1p images [Figs. 4(e)–4(h)]. It can be seen from the axial images (Fig. 5) that, although the degradation of 2p resolution is not pronounced, the 2p fluorescence signal [Fig. 5(a)] decreases faster than the 1p fluorescence signal [Fig. 5(b)].

In conclusion, the penetration depth of 2p excitation in imaging through a tissue medium is smaller than that of 1p excitation because of the lower signal level in the former. However, within the depth of detectable signal, 2p excitation leads to image resolution approximately two orders of magnitude higher than that under 1p excitation.

The authors acknowledge support from the Australian Research Council. One of the authors (A.K.) of the University of Twente, The Netherlands, spent his three-month study leave at Victoria University, Australia. Nicoleta Dragomir of Victoria University was partly involved in this work.

- ¹W. Denk, J. H. Strickler, and W. W. Webb, *Science* **248**, 73 (1990).
- ²V. E. Centonze and J. G. White, *Biophys. J.* **75**, 2015 (1998).
- ³S. Hell, *Bioimaging* **4**, 121 (1996).
- ⁴B. R. Masters, P. T. C. So, and E. Gratton, *Biophys. J.* **72**, 2405 (1997).
- ⁵S. P. Schilders and M. Gu, *Appl. Opt.* **38**, 720 (1999).
- ⁶Y. Guo, Q. Z. Wang, N. Zhadin, F. Liu, S. Demos, D. Calstru, A. Tirk-sliunas, A. Katz, Y. Bunansky, P. P. Ho, and R. R. Alfano, *Appl. Opt.* **36**, 968 (1997).
- ⁷W. Denk, K. Delaney, A. Gelperin, D. Kleinfeld, B. Strowbridge, D. Tank, and R. Yuste, *J. Neurosci. Methods* **54**, 151 (1994).
- ⁸W. Cheng, S. A. Prael, and A. J. Welch, *IEEE J. Quantum Electron.* **26**, 2166 (1990).
- ⁹S. Morgan, M. Khong, and M. Somekh, *Appl. Opt.* **36**, 1560 (1997).
- ¹⁰C. F. Bohern and D. R. Huffman, *Absorption and Scattering of Light by Small Particles* (J. Wiley, New York, 1983).
- ¹¹X. Gan, S. P. Schilders, and M. Gu, *J. Opt. Soc. Am. A* **15**, 2052 (1998).
- ¹²S. Pan, A. Shih, W. Liou, M. Park, J. Bhawalkar, J. Swiatkiewicz, J. Samarabandu, P. N. Prasad, and P. C. Cheng, *Scanning* **19**, 156 (1997).
- ¹³M. Gu, *Principles of Three-Dimensional Imaging in Confocal Microscopes* (World Scientific, Singapore, 1996).
- ¹⁴M. Gu, S. Schilders, and X. Gan, *J. Mod. Opt.* **47**, 2000 (1999).
- ¹⁵C. M. Blanca and C. Saloma, *Appl. Opt.* **37**, 8092 (1998).